

**Sensors****A Molecular Imaging Approach to Mercury Sensing Based on Hyperpolarized  $^{129}\text{Xe}$  Molecular Clamp Probe**

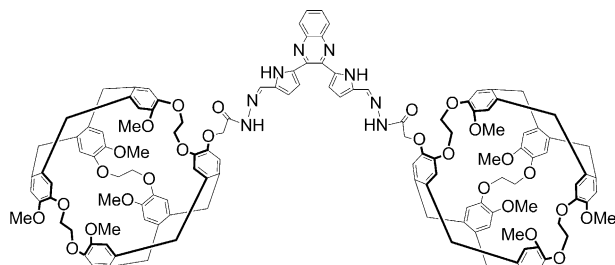
Qianni Guo,<sup>[a]</sup> Qingbin Zeng,<sup>[a]</sup> Weiping Jiang,<sup>[a]</sup> Xiaoxiao Zhang,<sup>[a]</sup> Qing Luo,<sup>[a]</sup> Xu Zhang,<sup>[a]</sup> Louis-S. Bouchard,<sup>[b]</sup> Maili Liu,<sup>[a]</sup> and Xin Zhou<sup>\*[a]</sup>

**Abstract:** Mercury pollution, in the form of mercury ions ( $\text{Hg}^{2+}$ ), is a major health and environmental hazard. Commonly used sensors are invasive and limited to point measurements. Fluorescence-based sensors do not provide depth resolution needed to image spatial distributions. Herein we report a novel sensor capable of yielding spatial distributions by MRI using hyperpolarized  $^{129}\text{Xe}$ . A molecular clamp probe was developed consisting of dipyrrolylquinoxaline (DPQ) derivatives and two cryptophane-A cages. The DPQ derivatives act as cation receptors whereas cryptophane-A acts as a suitable host molecule for xenon. When the DPQ moiety interacts with mercury ions, the molecular clamp closes on the ion. Due to overlap of the electron clouds of the two cryptophane-A cages, the shielding effect on the encapsulated Xe becomes important. This leads to an upfield change of the chemical shift of the encapsulated Xe. This sensor exhibits good selectivity and sensitivity toward the mercury ion. This mercury-activated hyperpolarized  $^{129}\text{Xe}$ -based chemosensor is a new concept method for monitoring  $\text{Hg}^{2+}$  ion distributions by MRI.

Mercury pollution remains a problem of global proportions perpetuated by the occurrence of natural geological events and the widespread use of mercury species in human activities.<sup>[1]</sup> A wide range of tools, such as  $\text{Hg}^{2+}$  ion chemosensors, have been developed to detect and monitor local mercury concentrations.<sup>[2]</sup> However, these methods are invasive and require close proximity of the sensor to the sample under study, making it impossible to obtain spatial distributions of  $\text{Hg}^{2+}$  ions within a system or region of interest. New methods are

needed to map the extent of mercury exposure and changes in its distribution over time. There are several methods to promote the sensitivity of NMR technology, such as CEST (chemical exchange saturation transformation) and hyperpolarization.<sup>[3]</sup> Herein we present a mercury-activated  $^{129}\text{Xe}$  molecular-clamp probe. The mercury sensor is minimally invasive, can be imaged with depth resolution, and its detection sensitivity as function of depth exceeds that of fluorescence-based sensors.<sup>[4]</sup> In this approach, the xenon nuclear spins are hyperpolarized, using the spin-exchange optical pumping (SEOP) technique, by several orders of magnitude compared to the Boltzmann population.<sup>[5]</sup> This leads to amplification of the NMR sensitivity by factors of more than 10 000 in high field (> 1 T), enabling sensitive detection of weak signals at very low concentrations.<sup>[6]</sup> When developing  $^{129}\text{Xe}$ -based biosensors, the main challenge is that Xe atoms are chemically inert, making it difficult to create Xe-substrate fusions for the localized delivery of Xe signals. Modern hyperpolarized  $^{129}\text{Xe}$  NMR sensing systems generally invoke two elements. The first is a binding site, which is affected by the ligand topology, the guest properties (ionic radius, charge, coordination number, hardness, etc.) and the nature of the solvent. The other element is the molecular-recognition mechanism. The Xe center is endowed with the capability of altering its chemical shift upon binding to report on the nature of the binding process.

Our sensor consists of dipyrrolylquinoxaline (DPQ) derivatives and two cryptophane-A cages. The DPQ derivatives act as cation receptors,<sup>[7]</sup> whereas cryptophane-A acts as a suitable host molecule for xenon.<sup>[8]</sup> The chemosensor **1** was designed like a molecular clamp that can clip the target ions in its clamp's cave, using DPQ as the basic molecular frame, pyrrole and the imine as the recognition site, and cryptophane-A as the Xe NMR signal reporter moiety (Scheme 1).



**Scheme 1.** Molecular structure of chemosensor **1**.

[a] Prof. Dr. Q. Guo, Q. Zeng, W. Jiang, X. Zhang, Prof. Dr. Q. Luo, Prof. Dr. X. Zhang, Prof. Dr. M. Liu, Prof. Dr. X. Zhou

Key Laboratory of Magnetic Resonance in Biological Systems  
State Key Laboratory of Magnetic Resonance and Atomic and Molecular Physics, Wuhan Center for Magnetic Resonance  
Wuhan Institute of Physics and Mathematics  
Chinese Academy of Sciences, Wuhan (P.R. China)  
E-mail: xinzhou@wipm.ac.cn

[b] Prof. Dr. L.-S. Bouchard  
Department of Chemistry and Biochemistry  
California NanoSystem Institute, The Molecular Biology Institute  
University of California, Los Angeles, CA 90095 (USA)

Supporting information and ORCID(s) from the author(s) for this article are available on the WWW under <http://dx.doi.org/10.1002/chem.201600193>.

Due to the change in electronic density of the chromophore induced by complexation, when the ionophore moiety is complexed to a metal ion, substantial changes in the absorption spectra can be observed.<sup>[9]</sup> Since the recognition site is now part of the chromophore, when conjugated with the cation in solution, the analytical potential of the system is greatly enhanced. The binding affinity of the sensor to the metal ion is controlled by the oxidation state of the nitrogen atoms of the clamp. As shown in Figure 1, absorptions of chemosensor **1** appeared at 292, 328, and 395 nm, respectively, in solution (v/v DMSO/H<sub>2</sub>O = 1:4). The absorbance intensity decreased gradually with an increase in Hg<sup>2+</sup> concentration (about 10<sup>-6</sup>–10<sup>-5</sup> M, linearly dependent coefficient  $R^2=0.9954$ ). With Hg<sup>2+</sup>/ligand mole ratio > 1:1, a clear red shift (up to 12 nm) was observed. The isosbestic point was observed at 466 nm. As Hg<sup>2+</sup> solution was added to the ligand solution, the absorbance intensity reached a minimum and did not exhibit significant changes beyond. The  $R^2$  value of chemosensor **1** was 0.9954, which was close to 1. The binding constant of the complex evaluated from the UV/Vis spectra was founded to be  $3.57 \times 10^5$ . The result for chemosensor **1** were consistent with the formation of a complex with 1:1 stoichiometry and Hg<sup>2+</sup>, similar to other reported DPQ-based chemosensors.<sup>[10]</sup>

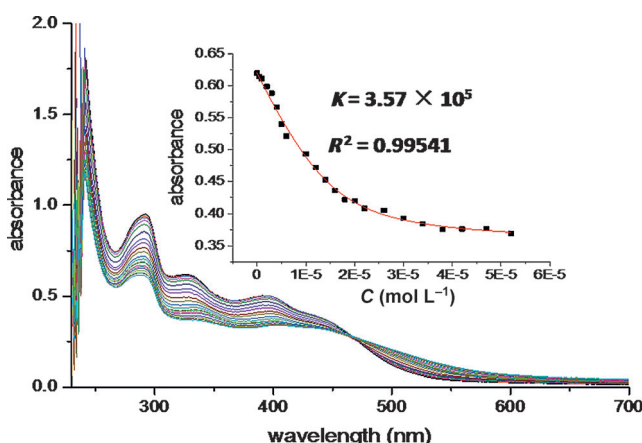


**Figure 1.** UV absorbance spectra of chemosensor **1** ( $3.0 \times 10^{-5}$  mol L<sup>-1</sup>) upon addition of Hg<sup>2+</sup>. Inset: the absorbance intensity at  $\lambda_{\text{max}}=328$  nm as function of mercury concentration.

To explore the utility of chemosensor **1** as an ion-selective chemosensor for Hg<sup>2+</sup>, control experiments were conducted with Mg<sup>2+</sup>, Ca<sup>2+</sup>, Zn<sup>2+</sup>, and Cd<sup>2+</sup> ions, at various concentrations (about 10<sup>-6</sup>–10<sup>-5</sup> M). We observed no obvious change in the absorbance intensity (Figure 2) when other cations (e.g., Mg<sup>2+</sup>, Ca<sup>2+</sup>, Zn<sup>2+</sup>, and Cd<sup>2+</sup>) were used instead of Hg<sup>2+</sup>. Since the sizes of Mg<sup>2+</sup>, Ca<sup>2+</sup>, Zn<sup>2+</sup>, and Cd<sup>2+</sup> are different, this suggests that the size of mercury(II) fits well within the molecule clamp's cave, indicating a prominent selectivity towards Hg<sup>2+</sup>.

<sup>129</sup>Xe NMR spectra successfully distinguished chemosensor **1** and its chelate in the presence of Hg<sup>2+</sup> ions (Figure 3). In the absence of Hg<sup>2+</sup> ions, the signal of xenon caged in chemosensor **1** (Xe@**1**) appeared at  $\delta=66.5$  ppm. The addition of Hg<sup>2+</sup> ions resulted an upfield increase of the chemical shift of Xe@**1**

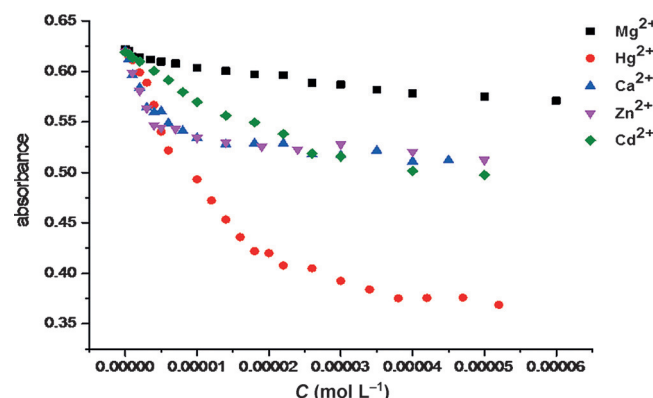


**Figure 2.** UV absorbance intensity of chemosensor **1** ( $3.0 \times 10^{-5}$  mol L<sup>-1</sup>) at  $\lambda_{\text{max}}=328$  nm as function of Mg<sup>2+</sup>, Hg<sup>2+</sup>, Ca<sup>2+</sup>, Zn<sup>2+</sup>, and Cd<sup>2+</sup> concentrations.

from  $\delta=66.5$  to 66.1 ppm ( $\Delta=38.6$  Hz). The <sup>129</sup>Xe NMR spectra also successfully distinguished chemosensor **1** and its chelate in the presence of Hg<sup>2+</sup> ions in a mouse serum solution. Without Hg<sup>2+</sup> ions, the signal of xenon caged in chemosensor **1** (Xe@**1**) appeared at  $\delta=68.4$  ppm in serum. The addition of Hg<sup>2+</sup> ions resulted an upfield increase of the chemical shift of xenon caged in chemosensor **1** (Xe@**1**) from  $\delta=68.4$  to 68.1 ppm ( $\Delta=30$  Hz). The chemical shift change of xenon caged in chemosensor **1** (Xe@**1**) showed a relative standard deviation at 2% (Figure S5 of the Supporting Information).

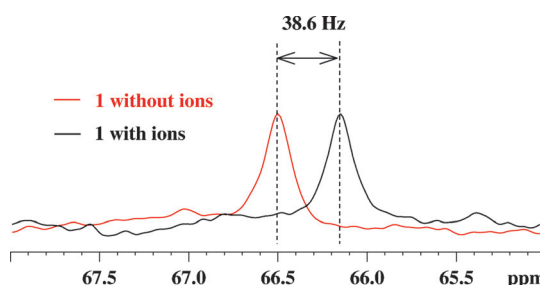
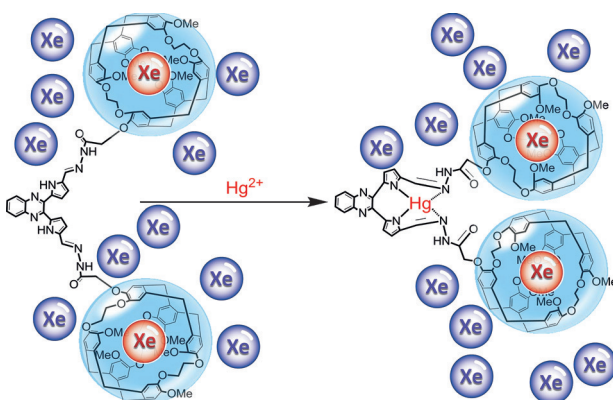


**Figure 3.** The upfield change of the NMR chemical shift of <sup>129</sup>Xe@**1** induced by Hg<sup>2+</sup>. The addition of Hg<sup>2+</sup> ions causes the chemical shift to decrease by nearly half a ppm.

The sensitivity threshold of the hyperpolarized <sup>129</sup>Xe NMR approach for Hg<sup>2+</sup> detection was assessed. Following the introduction of 1 atm of hyperpolarized xenon gas in the NMR tube, a Hg<sup>2+</sup> concentration of 1 μM could be readily detected (Figure S6 of the Supporting Information). The selectivity of this approach for Hg<sup>2+</sup> detection was also studied. The result was in agreement with the results reported by UV/Vis. When using Mg<sup>2+</sup>, Ca<sup>2+</sup>, Zn<sup>2+</sup>, and Cd<sup>2+</sup> instead of Hg<sup>2+</sup>, no obvious change in the signal of xenon caged in chemosensor **1** (Xe@**1**) could be observed. Compared with other hyperpolarized <sup>129</sup>Xe-based sensors of metal ions, the downfield change of chemical shift caused by electron-withdrawal effect of metal ions (e.g., the chemical shift signal of xenon caged in the reported Zn<sup>2+</sup> sensor changed from  $\delta=65.75$  to 67.2 ppm),<sup>[11]</sup> the upfield change of chemical shift of Xe@**1** was totally different. Since

design of this probe is totally different from our previous designed probe,<sup>[12]</sup> the change of chemical shift of Xe@1 is influenced not only by the electron-withdrawing effect of the metal ions, but also by the shielding effect of the two cryptophane-A cages. These results not only demonstrate that the Hg<sup>2+</sup> ions were indeed chelated with the DPQ moiety, but also suggest that the distance between the two cryptophane-A cages of chemosensor 1 is reduced after binding. When binding with Hg<sup>2+</sup> the molecular structure of chemosensor 1 turned from open to closed (Scheme 1). As the electron clouds of the two cryptophane-A cages overlap the shielding effect towards encapsulated Xe becomes important. The influence of shielding effects from electronic clouds of the two cryptophane-A cages overlapping was stronger than the deshielding effect of the electron-withdrawing effect of metal ions on the chemical shift of Xe@1. An upfield change of chemical shift of Xe@1 was induced.



**Scheme 2.** Conformational change of chemosensor 1 induced by its interaction with Hg<sup>2+</sup>. The blue bubbles represent electronic cloud of cryptophane-A. The red bubbles represent the caged Xe and the purple bubbles represent the free Xe.

To determine the binding mechanism and molecular structure changes of chemosensor 1 before and after interaction with Hg<sup>2+</sup> more precisely, a NOESY experiment was performed (Figure 4). It can be seen that two strong signals from brNH (broad peak of NH at 9.945 and 10.360 ppm) of the compounds vanish in the presence of the Hg<sup>2+</sup>. Since deprotonation is usually clear evidence of the formation of a conjugate bond, this result indicated that the two nitrogen atoms of brNH chelated with the Hg<sup>2+</sup> directly. The chelation was also confirmed by the chemical shift change of the quinoxaline CH. The chemical shift of the quinoxaline CH proton resonance is 7.198 ppm without Hg<sup>2+</sup>. With the addition of Hg<sup>2+</sup> the resonance is downfield shifted to 0.260 ppm. This indicated that the quinoxaline CH was deshielded, which appeared to be due to the deprotonation of brNH nitrogen atoms, and the direct bonding to the brNH nitrogen atoms directly. The chemical shift of the aromatic hydrogen atoms changed slightly, indicating that the cryptophane-A cages were far away from the binding sites. Also, the molecular structure change of chemosensor 1 caused a shielding effect of the aromatic hydrogen

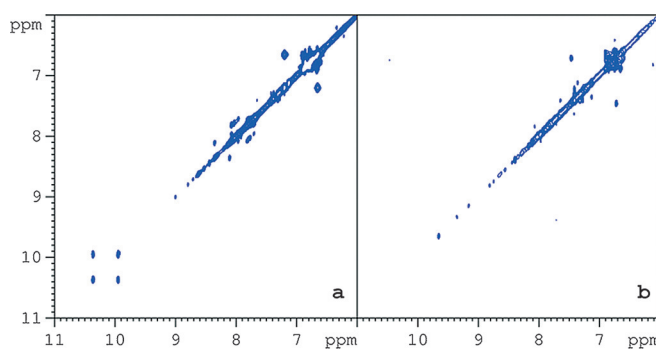


**Figure 4.** 2D  $^1\text{H}$ - $^1\text{H}$  NOESY spectra of the chemosensor 1 in the: a) absence, and b) presence of Hg<sup>2+</sup> ions. The experiments were performed at 20°C on a Bruker Avance III 600 NMR instrument equipped with a triple resonance clamp-probe. The mixing time for magnetization transfer by cross-relaxation was 500 ms. Solvent suppression was accomplished using WATERGATE before the acquisition to avoid signal loss from the exchangeable protons.

atoms that likely offset the electron-withdrawing effect of the Hg<sup>2+</sup>.

The change in chemical shift between the signals of encapsulated xenon in the absence and in the presence of Hg<sup>2+</sup> ions relative to the NMR linewidths was sufficient to enable spectroscopic MRI of these chemical species. Figure 5 images were obtained using a CSI method. Comparison between images a and b in Figure 5 shows that the Hg<sup>2+</sup> ions can be specifically detected and localized at low concentration in a short time.

These results demonstrate that highly sensitive and selective detection of Hg<sup>2+</sup> can be achieved with a simple molecular clamp chemosensor. Detection by MRI (Figure 5) and optical (Figure 1) methods is possible. The MRI method enables assessment of spatial distributions of mercury. This mercury-activated hyperpolarized  $^{129}\text{Xe}$ -based chemosensor is a new concept method for monitoring Hg<sup>2+</sup> ions.

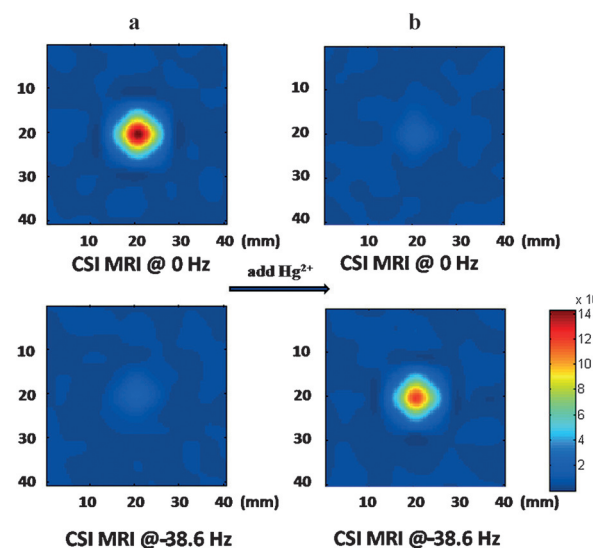


**Figure 5.** Chemical shift image (CSI MRI) of chemosensor 1: a) with, and b) without the addition of Hg<sup>2+</sup>.

## Acknowledgements

This work was supported by the National Natural Science Foundation of China (81227902, 21302217, and 21475147).

**Keywords:** hyperpolarized  $^{129}\text{Xe}$  • mercury • molecular clamp probe • molecular imaging • sensors

- [1] a) M. Nendza, T. Herbst, C. Kussatz, A. Gies, *Chemosphere* **1997**, *35*, 1875; b) D. W. Boening, *Chemosphere* **2000**, *40*, 1335; c) S. Ando, K. Koide, *J. Am. Chem. Soc.* **2011**, *133*, 2556–2566.
- [2] a) E. M. Nolan, S. J. Lippard, *Chem. Rev.* **2008**, *108*, 3443; b) D. G. Cho, J. L. Sessler, *Chem. Soc. Rev.* **2009**, *38*, 1647; c) D. T. Quang, J. S. Kim, *Chem. Rev.* **2010**, *110*, 6280; d) Q. Liu, J. Peng, L. Sun, F. Li, *ACS Nano* **2011**, *5*, 8040–8048.
- [3] a) E. Y. Chekmenev, K. W. Waddell, J. Hu, Z. Gan, R. J. Wittebort, T. A. Cross, *J. Am. Chem. Soc.* **2006**, *128*, 9849–9855; b) Y. Feng, T. Theis, X. Liang, Q. Wang, P. Zhou, W. S. Warren, *J. Am. Chem. Soc.* **2013**, *135*, 9632–9635; c) R. Trokowski, J. Ren, F. K. Kálmán, D. Sherry, *Angew. Chem. Int. Ed.* **2005**, *44*, 6920–6923; *Angew. Chem.* **2005**, *117*, 7080–7083; d) L. Schröder, T. J. Lowery, C. Hilly, D. E. Wemmer, A. Pines, *Science* **2006**, *314*, 446–449.
- [4] a) N. Dave, M. Y. Chan, P. Huang, B. D. Smith, J. Liu, *J. Am. Chem. Soc.* **2010**, *132*, 12668–12673; b) J. Chan, S. C. Dodani, C. J. Chang, *Nat. Chem.* **2012**, *4*, 973–984.
- [5] a) M. M. Spence, S. M. Rubin, A. Pines, S. Yao, F. Tian, P. G. Schultz, *Proc. Natl. Acad. Sci. USA* **2001**, *98*, 10654–10657; b) W. Happer, E. Miron, S. Schaefer, D. Schreiber, W. A. van Wijngaarden, X. Zeng, *Phys. Rev. A* **1984**, *29*, 3092–3110; c) X. Zeng, Z. Wu, T. Call, E. Miron, D. Schreiber, W. Happer, *Phys. Rev. A* **1985**, *31*, 260–278; d) T. G. Walker, W. Happer, *Rev. Mod. Phys.* **1997**, *69*, 629–642; e) X. Zeng, C. Wu, M. Zhao, *Chem. Phys. Lett.* **1991**, *182*, 538–540; f) X. Zhou, X. Sun, J. Luo, X. Zeng, M. Liu, M. Zhan, *Chin. Phys. Lett.* **2004**, *21*, 1501–1503.
- [6] a) A. Abragam, *Principles of Nuclear Magnetism*, Oxford University Press, New York, **1961**; b) P. Nikolaou, A. M. Coffey, M. J. Barlow, M. Rosen, B. M. Goodson, E. Y. Chekmenev, *Anal. Chem.* **2014**, *86*, 8206; c) P. Nikolaou, A. M. Coffey, L. L. Walkup, B. M. Guest, N. Whiting, H. Newton, S. Barcus, I. Muradyan, M. Dabaghyan, G. D. Moroz, M. S. Rosen, S. Patz, M. J. Barlow, E. Y. Chekmenev, B. M. Goodson, *Proc. Natl. Acad. Sci. USA* **2013**, *110*, 14150–14155.
- [7] L. Wang, X. Zhu, W. Wong, J. Guo, W. Wong, Z. Li, *Dalton Trans.* **2005**, 3235–3240.
- [8] a) J. M. Chambers, P. A. Hill, J. A. Aaron, Z. Han, D. W. Christianson, N. N. Kuzma, I. J. Dmochowski, *J. Am. Chem. Soc.* **2009**, *131*, 563–569; b) P. Berthault, G. Huber, H. Desvaux, *Prog. Nucl. Magn. Reson. Spectrosc.* **2009**, *55*, 35–60; c) E. Dubost, J. P. Dognon, B. Rousseau, G. Milanole, C. Dugave, Y. Boulard, E. Léonce, C. Boutin, P. Berthault, *Angew. Chem. Int. Ed.* **2014**, *53*, 9837–9840; *Angew. Chem.* **2014**, *126*, 9995–9998; d) S. Klippe, J. Döpfert, J. Jayapaul, M. Kunth, F. Rossella, M. Schnurr, C. Witte, C. Freund, L. Schröder, *Angew. Chem. Int. Ed.* **2014**, *53*, 493–496; *Angew. Chem.* **2014**, *126*, 503–506; e) C. Witte, V. Martos, H. M. Rose, S. Reinke, S. Klippe, L. Schröder, C. P. R. Hackenberger, *Angew. Chem. Int. Ed.* **2015**, *54*, 2806–2810; *Angew. Chem.* **2015**, *127*, 2848–2852.
- [9] a) H. Sakamoto, J. Ishikawa, S. Nakao, H. Wada, *Chem. Commun.* **2000**, 2395–2396; b) H. Ji, R. Dabestani, G. M. Brown, R. L. Hettich, *Photochem. Photobiol.* **1999**, *69*, 513–516; c) K. Wen, S. Yu, Z. Huang, L. Chen, M. Xiao, X. Yu, L. Pu, *J. Am. Chem. Soc.* **2015**, *137*, 4517–4524.
- [10] a) Y. Hu, Q. Li, H. Li, Q. Guo, Y. Lu, Z. Li, *Dalton Trans.* **2010**, *39*, 11344–11352; b) Q. Guo, C. Zhong, Y. Lu, C. Shi, Z. Li, *J. Inclusion Phenom. Macrocyclic Chem.* **2012**, *72*, 79–88.
- [11] N. Kotera, N. Tassali, E. Léonce, P. Berthault, T. Brotin, J. P. Dutasta, L. Delacour, T. Traoré, D. A. Buisson, F. Taran, S. Coudert, B. Rousseau, *Angew. Chem. Int. Ed.* **2012**, *51*, 4100–4103; *Angew. Chem.* **2012**, *124*, 4176–4179.
- [12] J. Zhang, W. Jiang, Q. Luo, X. Zhang, Q. Guo, M. Liu, X. Zhou, *Talanta* **2014**, *122*, 101–105.

Received: January 15, 2016

Published online on February 2, 2016